AN ILLUMINATION MODEL FOR TRANSLUCENT CONCRETE USING RADIANCE

Aashish Ahuja[1], Khalid M. Mosalam[2], and Tarek I. Zohdi[1]
[1]Department of Mechanical Engineering, University of California, Berkeley, USA
[2]Department of Civil Engineering, University of California, Berkeley, USA
email: aashishahuja@berkeley.edu, mosalam@berkeley.edu, zohdi@me.berkeley.edu

ABSTRACT

An alternative building envelope solution called 'Translucent Concrete' (TC) is investigated. It consists of optical fibers (OFs) embedded in concrete that can channel sunlight into the office building workspace. The paper details the following: 1) a ray tracing algorithm to simulate light transmission of TC panel under Perez-sky model, 2) developing an interface within *RADIANCE* to model OFs, and 3) applying Markov models for occupancy and light switching models to estimate reduction in lighting requirements for the simulated room. As an example, an office space is simulated by replacing its south-facing wall with TC. The ray tracing results are integrated with *RADIANCE* to calculate the illuminance in this space. It is observed from the studied office room example that 43.5% to 84% of lighting energy (spent between 8 am - 6 pm) can be saved annually by using TC panels containing 49 fibers per panel or 121 fibers per panel, respectively.

INTRODUCTION

The translucent concrete (TC) panel is developed as an alternative technology for capturing and delivering daylight into buildings that could reduce our dependence on artificial lighting and save electricity. The TC panel is considered as a part of the building envelope (*i.e.* walls or roof) since it satisfies requirements like (Mosalam et al., 2013): (a) Envelope behaving as a structural sub-system (b) Construction procedure is simple and scalable and (c) Movable and mechanized parts are avoided.

In this research, we use sunlight data from National Renewable Energy Laboratory for estimating the total sunlight incident in a location like Berkeley, CA. A ray tracer was developed in (Ahuja et al., 2014) for the purpose of computing the light transmitting capabilities of TC. This ray tracing software is integrated with *RADIANCE* (Ward, 1994) in this research for computing the illumination of the example room. Models for occupancy and light switching are used to estimate the annual savings in energy due to greater reliance on natural daylight than artificial lighting. This paper assesses the feasibility and limitations of a new translucent material in terms of energy savings for the building stakeholders.

LITERATURE REVIEW

In 2001, the first commercial form of TC was invented by Hungarian architect Aron Losonczi. It was a combination of optical fibers and concrete with fine aggregate but was used for decorative purposes. University of Detroit-Mercy developed translucent panels made of Portland cement and sand and reinforced with a small amount of chopped fiberglass. The primary focus of the TC technology has previously been on its aesthetic appeal and its application in artistic design. The authors are currently envisioning the use of TC as a structural building material. This entails that TC panels should be tested and simulated for light transmission, thermal properties, structural strength, hygrothermal effects and its impact on the entire building.

The occupant's presence over the year is estimated using an inhomogeneous Markov chain model. Prior to this model, most of the occupancy was derived from average user behavior without much emphasis on the randomness of every individual's behavior. This simplification, in handling occupancy data, failed to account for the changes in the behaviors observed for different days of the week, presence during weekends and other atypical behaviors like early departure or early arrivals. The Markov chain model described in (Page et al., 2008) is used in (Chapman et al., 2014) which replaces the fixed profile approach with a probability profile for presence. Field investigations on behavioral patterns of occupants have led to the development of light switching models. Interested readers are referred to (Hunt, 1979), (Reinhart and Voss, 2003), (Reinhart, 2004) and (Lindelöf and Morel, 2006) for understanding the interaction of occupants with the lighting systems (on arrival and thereafter) as a function of the work plane illuminance.

THEORY AND MODELING

Modeling light transmission through TC

Modeling the TC panel

For simulation purposes, a TC panel was modeled as a cuboid with dimensions 0.3 m×0.3 m×0.1 m as

shown in Figure 1. The transparency of the TC panel is varied by changing the volumetric ratio of optical fibers embedded in the concrete panel. Each optical fiber is a cylinder with a radius of 5 *mm*. The light travels in the core of the optical fibers which is made of PMMA (Poly-Methyl MethAcrylate). The core is surrounded by a thin layer of PF (Perfluorinated) polymer known as the cladding, which protects the core and allows light to propagate by total internal reflection (TIR) at the core-cladding interface.

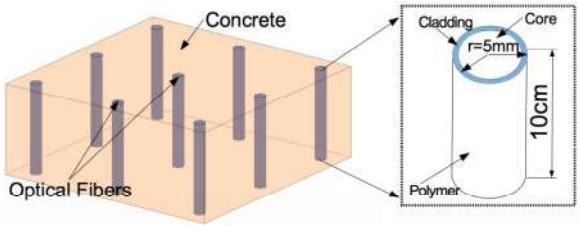

Figure 1 A computational model of TC panel with embedded optical fibers (illustration not to scale)

Transmission behavior of optical fibers

A ray of light incident on an optical fiber in the TC panel undergoes three noticeable light phenomena: reflection and refraction on its top surface and TIR along the inside walls of the fiber. The part of light reflected after striking the top of optical fibers is given as (see (Zohdi, 2012) for derivation):

$$R = \frac{1}{2}\left(\left(\frac{\frac{\hat{n}}{\hat{\mu}}cos\theta_i - \sqrt{\hat{n}^2 - \sin^2\theta_i}}{\frac{\hat{n}}{\hat{\mu}}cos\theta_i + \sqrt{\hat{n}^2 - \sin^2\theta_i}}\right)^2 + \left(\frac{cos\theta_i - \frac{1}{\hat{\mu}}\sqrt{\hat{n}^2 - \sin^2\theta_i}}{cos\theta_i + \frac{1}{\hat{\mu}}\sqrt{\hat{n}^2 - \sin^2\theta_i}}\right)^2\right) \quad (1)$$

where $0 \leq R \leq 1$ for an angle of incidence θ_i, $\hat{\mu} = \mu_t/\mu_i = 1$ ($\hat{\mu}$ is the ratio of magnetic permeabilities for transmission and incident media) and $\hat{n} = n_t/n_i$ ($\hat{n}$ *is* the ratio of refractive indices for transmission and incident media). The other part of light that is refracted into the optical fibers may or may not undergo TIR. For the TIR to occur within an optical fiber:

$$n_{core} \sin\theta_i > n_{cladding} \quad (2)$$

where n_{core} and $n_{cladding}$ are the refractive indices for the core and cladding materials of the optical fiber, respectively. Light rays that do not obey the condition in EQUATION (2) are converted to heat within the fiber. Light is dissipated inside the core of the fibers due to scattering (Jones, 1997) and absorption (Kaino, 1985). Light losses due to these factors were observed to be significant only in spectra falling outside the visible range (380 *nm* - 780 *nm*) and were thus ignored in this research.

Ray tracing

Ray tracing methods begin by representing wavefronts as an array of discrete rays. Geometrically, one proceeds by tracking each ray as it changes trajectories. On encountering a surface, the intersection point is either determined analytically (in case the surface geometry is simple such as sphere or polygon) or using some numerical method, like Newton's method. Next, Fresnel's laws are applied at the intersection point and the outgoing ray (reflected or refracted ray) is calculated. Ray-tracing methods, in general, are suited for the computation of scattering in systems that are difficult to mesh/discretize. It is assumed that the length scale of the surface features is large enough relative to the wavelength of sunlight ($280\ nm \leq \lambda \leq 4000\ nm$) (Zohdi, 2012).

The surface roughness at the two ends of the fiber can change the incidence angle of a light ray. The interaction of light ray with surface asperities is modeled as a random variable with two states, say 0 and 1, and upon having say '1', a new normal is randomly generated which is considered to be orthogonal to the irregularity. The transmission behavior inside the fiber is unaffected which is computed using the ray tracing method.

Modified Perez-sky model

The Perez model for sky (Perez et al., 1987) is used to estimate the global illuminance (*lux*) on a tilted surface. The global illuminance (G) on a tilted surface depends on direct beam (G_n) and diffuse (G_d) components of sunlight illuminance which yields:

$$G = G_n \cos\theta + G_d \quad (3)$$

where θ is the angle between the sun direction and normal to the panel surface. The diffuse solar radiation (G_d) on a tilted surface is the sum of the following components (also shown in Figure 2):

1. Isotropic radiation which is uniformly distributed over the sky vault.
2. Radiations from circumsolar disk and sky horizon which causes anisotropic distribution of diffused light.

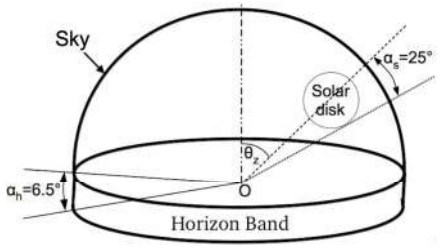

Figure 2 Description of Perez circumsolar radiation and horizon radiation band

The circumsolar disk, which subtends a half angle of 25° around the sun, is produced from forward scattering by aerosols and air molecules. A bright band of 6.5° elevation develops near the horizon because of sunlight retroscattering. The Perez sky and global illuminance in EQUATION (3) are

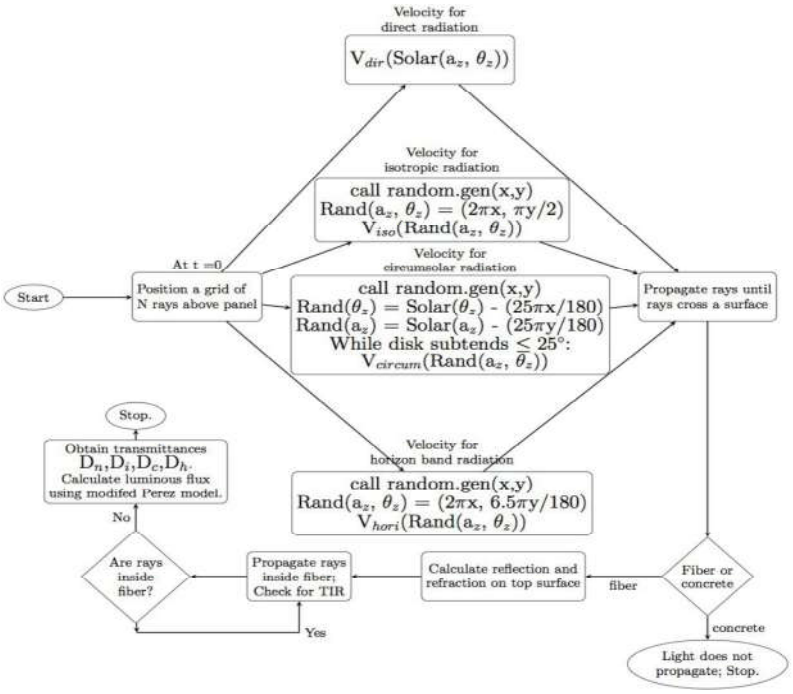

Figure 3 Algorithm for calculation of the total flux emitted from a TC panel. The velocities ($\boldsymbol{V_{dir}, V_{iso}, V_{circum}, V_{hori}}$) refer to the speed and direction of N groups of light rays that are projected towards TC from their source of generation i.e. direct, isotropic, circumsolar and horizon band radiation, respectively.

modified to include scalar factors which are used to calculate the light transmitted through a tilted TC panel (Ahuja et al., 2014). The resulting equations are

$$G' = D_n G_n cos\theta + G'_d$$
$$G'_d = G_d(0)[D_1(1-F_1)\frac{1+cos\beta}{2} + D_c F_1 \frac{cos\theta}{cos\theta_z} + D_h F_2 sin\beta] \quad (4)$$

where

$$F_1(\epsilon) = f_{11} + f_{12}\Delta + f_{13}\theta_z$$
$$F_2(\epsilon) = f_{21} + f_{22}\Delta + f_{23}\theta_z \quad (5)$$

and

$$\Delta = \frac{mG_d(0)}{G_{etr}}, \epsilon = \frac{G_d(0) + G_n(0)}{G_d(0)} \quad (6)$$

In the above relations, $G_d(0)$ and $G_n(0)$ refer to diffused and direct beam illuminations, respectively, on a horizontal plane. m stands for the atmospheric air mass and G_{etr} is the extraterrestrial solar illumination. G' and G'_d represent the global and diffused illuminances, respectively, collected on a surface adjoining and parallel to the TC panel. D_n, D_i, D_c, D_h are the averaged panel transmittance ratios for their respective global illumination components. The diffuse illuminance, G'_d is also dependent on sky brightness factor, Δ, atmospheric clearness, ϵ, and zenith angle, θ_z. The coefficients f_{ij} are dependent on ϵ as given in (Perez et al., 1987). Finally, G' and G'_d are multiplied by the area of the TC panel (0.09 m^2 in this case-study) to give the total luminous flux (in lm) value. A detailed algorithm for ray tracing using Perez sky model is given in Figure 3.

Illumination calculations over a work plane

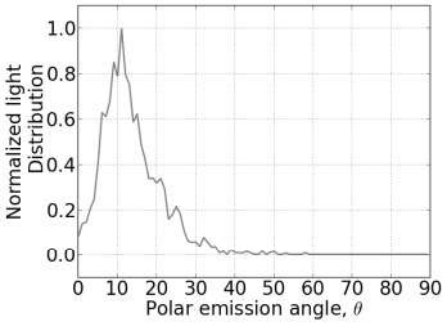

Figure 4 Normalized light distribution exiting from the fiber into the room.

The calculations are executed in the far field of the optical fiber, where the crossing of rays (caustics) is negligible and the illumination distribution has the form of the intensity distribution. The *RADIANCE* software can model customized luminaires and define the luminous intensity distribution for calculating illuminance at different points inside the room. The optical fiber is a point source that emits diffused light according to the transmission curve illustrated in Figure 4, calculated using ray tracing. It is noted that the normalization in Figure 4 is with respect to the maximum light transmitted for any polar angle, θ.

For a total light output of Φ *lm*, a large imaginary sphere is constructed around the optical fiber end of graph radius 5 *mm*. The sphere is divided into 180

sections of the (C0 - C180) plane such that each section subtends an elevation angle of 1° and an azimuth angle of 2π. The light output, Φ, is expressed according to (Wandachowicz, 2004) as

$$\Phi = \sum_{i=0}^{179} \Delta\Phi_i = \sum_{i=0}^{179} I_{c(\Delta\omega_i)} \Delta\omega_i \quad (7)$$

where $I_{c(\Delta\omega_i)}$ is the average luminous intensity emitted into the solid angle, $\Delta\omega_i$ expressed as

$$\Delta\omega_i = 2\pi(\cos i - \cos(i+1)) \quad (8)$$

Now, from the transmission curve in Figure 4, dependence between the different $\Delta\Phi_i$ can be established. The largest fraction of light rays exiting an optical fiber passes the section formed by angles {11°, 12°}. Let the corresponding light flux passing through this section be $\Delta\Phi_{11} = v_{11}\Phi$ where $v_{11} = 1$. Then, proportionally, $\Delta\Phi_0 = v_0\Phi$, $\Delta\Phi_1 = v_1\Phi$, and $\Delta\Phi_{i=90,91,\ldots,179} = 0$ since light is only radiated by the fiber tip to all sections between 0° and 90°. EQUATION (7) is reduced to

$$\Phi = \Phi_0(v_0 + v_1 + \cdots + 1 + \cdots + v_{89}) \quad (9)$$

$$\Phi_0 = \frac{\Phi}{\sum_{i=0}^{89} v_i} \quad (10)$$

$$\Delta\Phi_i = \frac{v_i\Phi}{\sum_{i=0}^{89} v_i} \quad (11)$$

and using EQUATION (8), assuming luminous intensity, $I_{c(\Delta\omega_i)}$, is uniform in each section, we get

$$I_{c(\Delta\omega_i)} = \frac{\Delta\Phi_i}{\Delta\omega_i} = \frac{v_i\Phi}{\Delta\omega_i \sum_{i=0}^{89} v_i} \quad (12)$$

The *RADIANCE* software uses two files to define the geometry and material, and the luminous intensity distribution of the optical fibers. The *RADIANCE* function *ies2rad* is used to prepare the luminous intensity distribution table for the optical fibers.

Algorithm for illumination calculations

The illumination on a workplane is calculated in *RADIANCE* using the algorithm shown in Figure 5. The first two steps of the algorithm are described in the previous section. The luminous flux values collected over the year are stored in a tabulated form and loaded into *RADIANCE*. A room is prepared in the software environment with one wall designed using TC panels. Each optical fiber in the panel is modeled as a separate luminaire which emits light into the room following the trend given in Figure 4. After assigning material properties to the surfaces of the room, the illumination is estimated at different points on the workplane located at the typical 0.8 m above the floor level.

Lighting controls

The simulated occupancy patterns are tied with the use of manual controls by the user. For this, we use multiple models that simulate the switching actions of users for different events. The probabilistic curve for switch-on at arrival shown in Figure 6 was adapted from (Hunt, 1979). The model was developed using time-lapse photography to emulate the occupant's switch-on action at arrival in the room. It is also observed that the user seldom operates switches while he/she has been present for sometime in the room. This predicts the occupants' intermediate actions for switch-on and switch-off (Lindelöf and Morel, 2006) as shown in Figure 7 and Figure 8, respectively. For all the light-switching models, it is observed that the occupants' actions are a function of the minimum illuminance received on the workplane. It should be noted that in (Lindelöf and Morel, 2006), the occupants switched on the lights before illuminance could drop to zero. Therefore, in this study, it was assumed that the intermediate switch-on and switch-off probabilities are 1.0 and 0.0, respectively, for zero illuminance.

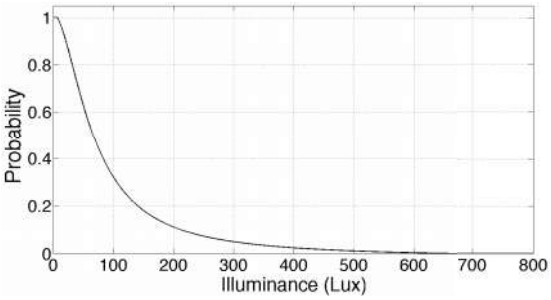

Figure 6 Probabilistic curve for switch-on at arrival

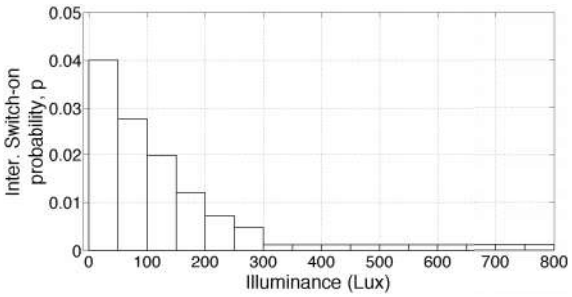

Figure 7 Intermediate switch-on (for illuminance=0, p=1.0)

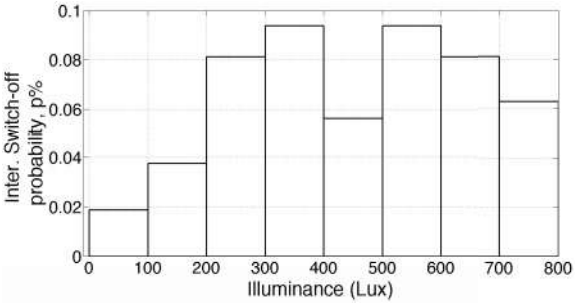

Figure 8 Intermediate switch-off (for illuminance=0, p=0.0)

Occupancy model

The state of presence within a building is a necessary condition for being able to quantify the occupant's interaction with lighting controls during the day. The

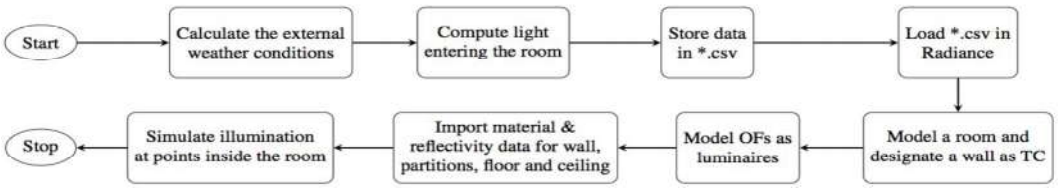

Figure 5 Algorithm for calculating illuminance due to TC in RADIANCE

prediction of an occupant presence in a workspace at particular time is a random event which is based on his/her average occupancy profile and mobility (how often he/she moves in and out of the room). The average occupancy profile and mobility were prepared using occupancy data collected over time and then using this data to train a time-inhomogeneous Markov chain model. Since the occupant exhibits only two states i.e. either present (state 1) or absent (state 0), the construction of the model is straightforward as illustrated in Figure 9. A number is randomly drawn between '0' and '1' for each state (presence or absence) and compared with values of transition (i.e. T00, T01, T11, or T10 given in Figure 9), to select the event that occurs in the next step. The algorithm is described using a flowchart given in Figure 10.

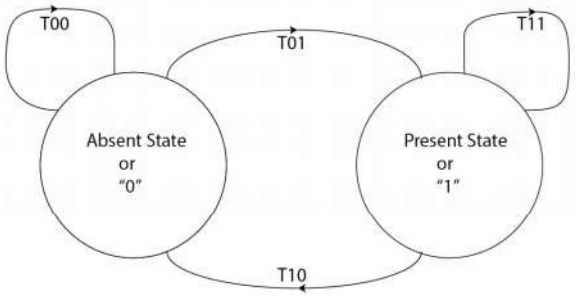

Figure 9 Time-inhomogeneous Markov chain model for occupancy.

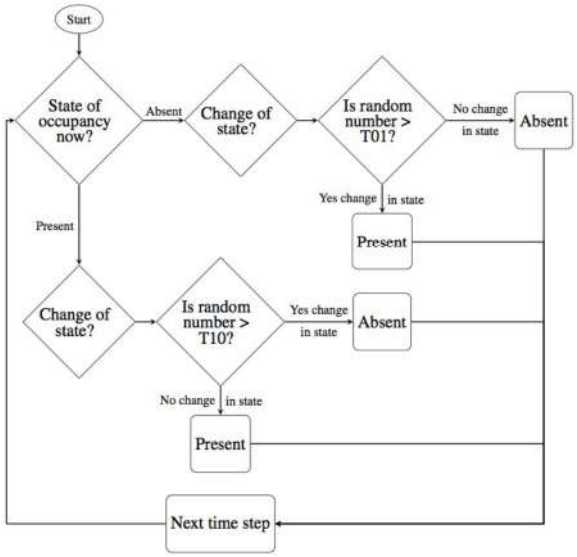

Figure 10 Occupancy model algorithm proposed by (Page et al., 2008) and used in this study

The Markov chain simulations produce a randomized time series of the presence (or absence) of occupant in the workspace. In this paper, a lab space in Berkeley was designated to train the occupancy model. The space is being shared by three occupants, two of whom are university students and the other occupant is part of the lab staff. The occupants' hourly presence is recorded for over three months (Aug - Nov 2014) continuously to generate their averaged occupancy profile for each day of the week and estimate their mobility in the lab during the semester. The occupancy data is collected using UC Berkeley's indigenous network of wireless sensors and actuators for monitoring AC energy usage. The entire architecture is called *ACme*.

Pseudo code and assumptions for energy savings estimator

Algorithm 1 Energy Savings Estimator

Input: Ray Tracing : *Calculate* Φ
Input: Workplane illuminance is calculated
save $\leftarrow 0$
for 1 to 100 **do**
  Generate: Annual Occupancy Profile
  for (1 to 365 days) **do**
    switch $\leftarrow 0$
    occ_{i-1} (at 8 a.m.) $\leftarrow 0$
    $T = 8\ a.m.$
    while ($T < 6\ p.m.$) **do**
      $illum \leftarrow WorkplaneIlluminance$
      $occ_i \leftarrow CurrentOccupancy$
      if occ_{i-1} and occ_i is 0 **then**
        switch $\leftarrow 0$
      else if occ_i is 1 **then**
        if occ_{i-1} is 0 **then**
          $switch \leftarrow SwitchOnAtArrival$
          if *switch* is 0 **then**
            save++
        else if occ_{i-1} is 1 and *switch* is 1 **then**
          $switch \leftarrow SwitchOnInter$
          if *switch* is 0 **then**
            save++
        else
          $switch \leftarrow SwitchOffInter$
          if *switch* is 0 **then**
            save++
      T += 1/2 *hr*
Savings per occupant is calculated as:
$LuminaireRating \times save/100(kW) \times 1/2(hr)$

The pseudo code for energy savings estimator is presented in Algorithm 1. The algorithm begins with the precondition that illuminance on the workplane for each occupant is available. Using Markov chain model, the algorithm generates a randomized annual occupancy profile. The switching models based on illuminance values and the occupancy status (i.e. Present or Absent) at the current moment decides whether the user prefers artificial lighting or sunlight.

If he/she relies on daylight, then the event contributes to energy savings before decision is made in the next time step. The total number of such events occurring over the year is recorded and the same process is repeated for 99 other random occupancy profiles of the same user. Total energy savings lump sum is simply the energy offset (in *kWh*) during the year when the occupant did not use electric lighting.

Long absences at work could not be modeled with the limited occupancy data available at the time of writing this paper. The switch-off probability at departure was excluded from the lighting performance model. It was assumed that the lights had occupancy sensors which switched off automatically as soon as the occupant left his/her space. Moreover, each occupant is supposed to have access to a lighting switch to controlling the illuminance on his/her desk.

Luminaire Rating is the power consumed by electrical lighting to illuminate the desk of an occupant. The expression for savings per occupant given in *Algorithm 1* is averaged over 100 profiles and converted to units of *kWh* by dividing it by 2.

Case study for illumination in an office room

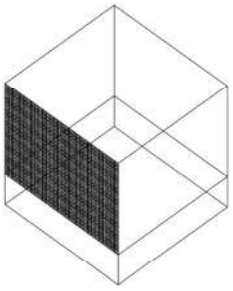

Figure 11 Wireframe model of lab with South-facing vertical TC wall

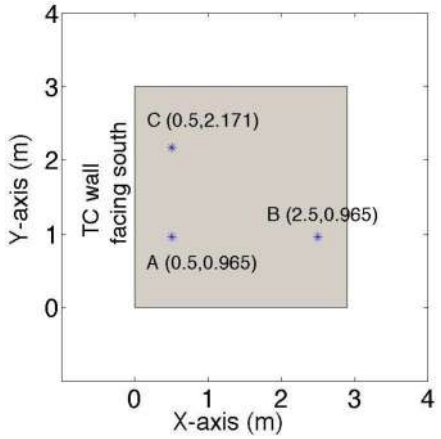

Figure 12 Workplane and positions A, B and C

Since we are only interested in the energy savings incurred over the day, we restrict our daily calculations to the time periods of 8 am – 6 pm local time (considering daylight savings). The lab room has a floor area of 3 m × 2.895 m with a ceiling height of 3.2 m. A workplane is constructed at 0.8 m above the floor over which illumination is calculated. The South-facing wall of the lab above the workplane height is con- structed with TC panels as shown in Figure 11. A total of 80 TC panels (panel size is 0.30 m × 0.30 m × 0.10 m) are used to span the required wall area. All the surfaces in the room are white and reflect 60% of the total light incident on them that is usually the higher limit of wall surface reflectivity as found in literature (den Ouden and Steemers, 2012). The students in the lab are very mobile often leaving their lab to attend classes, meetings or breaks while the staff member's work is more sedentary. Each occupant can occupy one of the three positions (*A*, *B* or *C)* marked in Figure 12. Thus, we simulate six positional arrangements for occupants 1, 2 and 3 and observe the energy saved in each case.

RESULTS AND DISCUSSIONS

The proposed façade subsystem contains multimode optical fibers that shields occupants from direct glare by light dispersion (Ghatak and Thyagarajan, 2000). The first simulation calculates the average amount of light (in *lm*) channeled by each fiber of the TC panel into the room. For this research, the dimensions and the geometry of a TC panel built in UC Berkeley are chosen as the representative element. A South-facing TC panel is simulated with exterior conditions imported from TMY (Typical Meteorological Year) data file for Oakland, California, which experiences the same weather conditions as Berkeley. The panel with a fiber volumetric ratio of 10.56% is simulated for angles {0°, 30°, 60°, 90°} tilted with respect to a vertical plane. Both Figure 13 and Figure 14 use different metrics to compare the effects of the tilt angles of the TC panel over the year. From the graphs, it is observed that a tilt angle, β^*=60°, transmits the maximum luminous flux through the TC panel.

The average flux output for one fiber is loaded into *RADIANCE*. The South-facing TC wall consists of panels that have either 121 optical fibers per panel (vol. ratio of 10.56%) or 49 optical fibers per panel (vol. ratio of 4.28%), arranged regularly. The illuminance is calculated at positions *A*, *B* and *C* for a wall tilted at angles 0° (conventional wall inclination) as shown in Figure 11 and 60° (case of maximum light flux output) as given in Figure 15. Illuminance simulations are carried out daily for the entire year using an interval of 30 *min* between 8 a.m. and 6 p.m. (local time). We use average occupancy profile for each occupant derived from three months of data (*e.g.* Figure 16 shows occupancy profiles for the three occupants used in this study). Using Markov chain model as described previously, we were able to generate several random profiles for the entire year for each occupant. The profiles are loaded into the code that executes Algorithm 1 and

calculates the energy savings for each of the the six combinations in positions that the three occupants can assume. In an office, the minimum amount of light on the working plane enforced by the building code (Section 9, ASHRAE Standard 90.1.2007) is 400 *lux*. Three similar T8 Fluorescent tubes consuming a total of 96 *W* are used to produce the required illumination level. Thus, by constructing a TC wall, one can expect savings in energy (*kWh*) for the several cases discussed here as listed in *Table 1*.

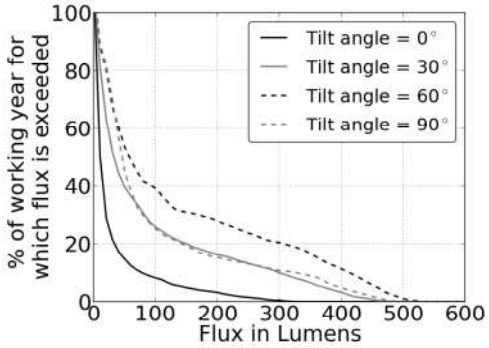

Figure 13 Luminous flux availability as percentage of the year such that flux value is exceeded

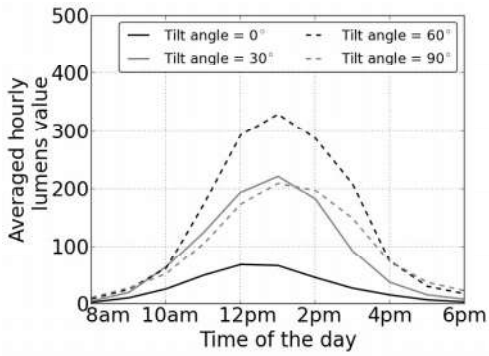

Figure 14 Average luminous flux calculated for each hour of the whole year

From the results, we observe that *Cases* 3 and 4 are slightly better suited for the lab. This refers to the case when occupant 2 occupies position *A*, and occupant 1 or occupant 3 either fill up position *B* or *C*. A TC wall tilted at 60° (TC #3 and #4) performs better than a vertical TC wall (TC #1 and #2) by saving a maximum of 26% more energy over the entire year. Though constructing a wall tilted at an angle of 60° might be impractical, we plan to explore optical fibers outfitted with concentrators and lenses that will be able to capture sunlight at extended times of the sun path. The TC wall containing panels with 49 optical fibers per panel has a fiber volumetric ratio which is 60% lower than the panel containing 121 fibers per panel. It is shown that the average savings with a vertical TC wall with 49 fibers per panel is only reduced by about 22% as compared to a wall with a higher volumetric ratio, *i.e.* 121 fibers per panel.

Any change in the volumetric ratio of fibers affects the structural strength of the wall, heat transmissivity and resistance to water penetration. This study will be used to decide the optimum fiber ratio in concrete that can maximize the thermal comfort of the occupants while providing sufficient daylight.

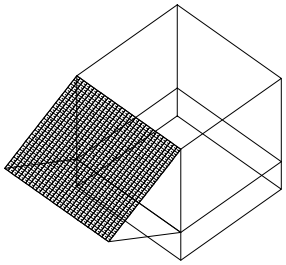

Figure 15 TC wall tilted at 60°

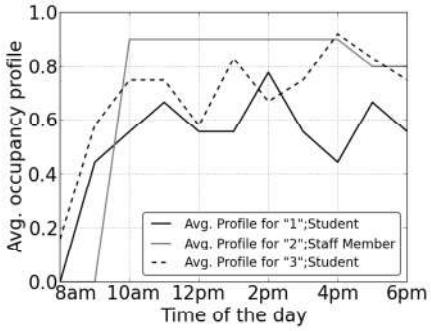

Figure 16 Avg. profile for occupants on Monday

CONCLUSIONS & LIMITATIONS

The TC panels have the distinct property of daylight transmission, which makes them useful for energy-efficient building envelopes. Using simulations, the functionality of TC in reducing the consumption of electricity is clearly demonstrated. This paper presents a method to estimate the expected energy savings after installing the TC walls in a building. This will help in quickly analysing the performance of the wall in different locations, which allows the designer to make design decisions, *e.g.* regarding the volumetric ratio of fibers and the orientation of the wall during construction. As a future extension of the study, the authors would experimentally test the performance of TC walls to validate the algorithm presented in this research. Also, additional data is being collected to predict the occupancy of lab users more accurately. This will provide a closer estimate of the actual energy saved during the year. Other features of the TC wall, *e.g.* using light concentrators, are under investigation using the same algorithm presented in this paper.

ACKNOWLEDGEMENTS

The occupancy model was provided courtesy of Dr. Darren Robinson and Mr Jacob Chapman. The presented research is funded by the Republic of Singapore's National Research Foundation through a grant to the Berkeley Education Alliance for Research in Singapore (BEARS)

Table 1 Savings in energy for different cases. Column 2 and Column 3 represents the performances of vertical TC walls containing panels with 49 and 121 fibers, respectively; Column 4 and Column 5 gives performance results for TC walls tilted at 60° to the vertical and containing panels with 49 and 121 fibers, respectively. The last column shows the amount of lighting energy used if the room only had opaque walls.

Positional arrangement of occupants (1, 2 and 3)	TC #1	TC #2	TC #3	TC #4	Max. potential energy savings
Case 1 (*A*, *B* and *C*)	65	100	107	129	154
Case 2 (*A*, *C* and *B*)	64	97	106	129	154
Case 3 (*B*, *A* and *C*)	67	101	107	129	154
Case 4 (*B*, *C* and *A*)	67	101	107	129	154
Case 5 (*C*, *A* and *B*)	64	99	106	129	154
Case 6 (*C*, *B* and *A*)	65	100	107	129	154

for the Singapore-Berkeley Building Efficiency and Sustainability in the Tropics (SinBerBEST) Program. BEARS has been established by the University of California, Berkeley as a center for intellectual excellence in research and education in Singapore. The authors would like to thank people in CREST, Cory Hall, Berkeley, CA for their cooperation in providing the sensor data, Mr Pierre Lemarchand for his assistance with RADIANCE, Ms Nuria Casquero Modrego and Mr Alex Mead for their feedback on this study.

REFERENCES

Ahuja, A., Mosalam, K. M., and Zohdi, T. I. (2014). "Computational Modeling of Translucent Concrete Panels." Journal of Architectural Engineering, (In press and available online).

Chapman, J., Siebers, P. O., and Robinson, D. (2014). "Coupling multi-agent stochastic simulation of occupants with building simulation." In "Proceedings of the 2014 Building Simulation and Optimization Conference," UCL, London, UK.

den Ouden, C. and Steemers, T. C. (Eds.). (2012). Building 2000: Volume 2 Office Buildings, Public Buildings, Hotels and Holiday Complexes. Springer Science & Business Media.

Ghatak, A. and Thyagarajan, K. (2000). Optical Waveguides and Fibers.

Hunt, D. (1979). "The Use of Artificial Lighting in Relation to Daylight Levels and Occupancy." Building and Environment, 14(1): 21–33.

Jones, W. (1997). "Linear Optical Properties of organic solids." In "Organic molecular solids: Properties and applications.", CRC Press.

Kaino, T. (1985). "Absorption losses of low loss plastic optical fibers." Japanese journal of applied physics, 24(12R).

Lindelöf, D. and Morel, N. (2006). "A field investigation of the intermediate light switching by users." Energy and Buildings, 38(7): 790–801.

Mosalam, K., Casquero-Modrego, N., Armengou, J., Ahuja, A., Zohdi, T., and Huang, B. (2013). "Anidolic Day-Light Concentrator in Structural Building Envelope." In "First Annual International Conference on Architecture and Civil Engineering (ACE 2013)," Singapore.

Page, J., Robinson, D., Morel, N., and Scartezzini, J. L. (2008). "A generalised stochastic model for the simulation of occupant presence." Energy and buildings, 40(2): 83–98.

Perez, R., Seals, R., Ineichen, P., Stewart, R., and Menicucci, D. (1987). "A new simplified version of the Perez diffuse irradiance model for tilted surfaces." Solar energy, 39(3): 221–231.

Reinhart, C. and Voss, K. (2003). "Monitoring manual control of electric lighting and blinds." Lighting Research and Technology, 35(3): 243–260.

Reinhart, C. F. (2004). "Lightswitch-2002: a model for manual and automated control of electric lighting and blinds." Solar Energy, 77(1): 15–28.

Wandachowicz, K. (2004). "Calculation of Luminaires Using Radiance." In "3rd International RA- DIANCE Workshop," Fribourg, Switzerland.

Ward, G. J. (1994). "The RADIANCE lighting simulation and rendering system." In "Proceedings of the 21st annual conference on Computer graphics and interactive techniques," pages 459–472.

Zohdi, T. I. (2012). "Modeling and simulation of the optical response rod-functionalized reflective surfaces." Computational Mechanics, 50(2): 257–268.